ACS NANO
Cite This: ACS Nano XXXX, XXX, XXX−XXX
www.acsnano.org

ARTICLE

# High-Power Aqueous Zinc-Ion Batteries for Customized Electronic Devices

Chanhoon Kim,[§,#] Bok Yeop Ahn,[†,‡,#] Teng-Sing Wei,[‡] Yejin Jo,[∥] Sunho Jeong,[∥] Youngmin Choi,[∥] Il-Doo Kim,[*,§] and Jennifer A. Lewis[*,†,‡]

[§]Department of Materials Science and Engineering, Korea Advanced Institute of Science and Technology, 291 Daehak-ro, Guseong-dong, Yuseong-gu, Daejeon 34141, South Korea

[†]Wyss Institute for Biologically Inspired Engineering, Harvard University, 3 Blackfan Circle, Boston, Massachusetts 02115, United States

[‡]John A. Paulson School of Engineering and Applied Sciences, Harvard University, 52 Oxford Street, Cambridge, Massachusetts 02138, United States

[∥]Division of Advanced Materials, Korea Research Institute of Chemical Technology, 176 Gajeong-dong, Yuseong-gu, Daejeon 34114, South Korea

Supporting Information

**ABSTRACT:** **Wireless electronic devices require small, rechargeable batteries that can be rapidly designed and fabricated in customized form factors for shape conformable integration. Here, we demonstrate an integrated design and manufacturing method for aqueous zinc-ion batteries composed of polyaniline (PANI)-coated carbon fiber (PANI/CF) cathodes, laser micromachined zinc (Zn) anodes, and porous separators that are packaged within three-dimensional printed geometries, including rectangular, cylindrical, H-, and ring-shapes. The PANI/CF cathode possesses high surface area and conductivity giving rise to high rate (~600 C) performance. Due to outstanding stability of Zn-PANI batteries against oxygen and moisture, they exhibit long cycling stability in an aqueous electrolyte solution. As exemplar, we demonstrated rechargeable battery packs with tunable voltage and capacity using stacked electrodes that are integrated with electronic components in customized wearable devices.**

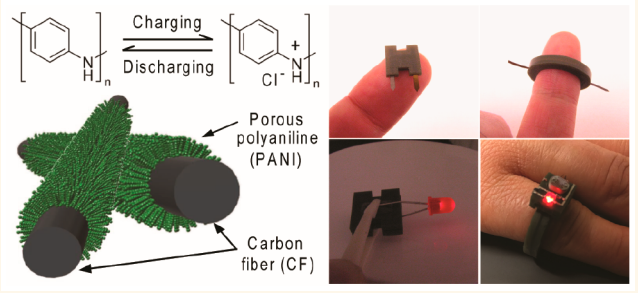


**KEYWORDS:** *aqueous zinc-ion batteries, 3D printing, polyaniline, carbon fiber mat, shape conformal batteries, wearable electronics*

Rechargeable batteries with arbitrary form factors may find broad application in customized electronics, soft robotics, smart sensors, and wearable devices.[1−13] Typically, these devices must be designed around the power source, which poses significant design constraints since commercial batteries are only available in a limited number of simple shapes, that is, coin, prismatic, cylindrical, and pouch cells. However, if one could create batteries in any desired shape or size, the design space would be nearly unlimited.[14−21]

Toward this objective, Kwon *et al.* recently created cable-type lithium-ion batteries (LIBs) by packaging cell components in a plastic tube.[16] This approach enables the production of cells in small diameters (~3 mm) with bendable and configurable motifs, but their shapes remain intrinsically limited to one-dimensional (1D) cables. Xu *et al.* produced stretchable LIBs in planar geometries packaged and sealed in a thin elastomeric substrate coupled with self-similar serpentine interconnects.[17] Lee and co-workers packaged LIBs in thin plastic substrates using a solid-state composite electrolyte (SCE)[20] and demonstrated their integration into an eyeglass frame along with other simple shapes. However, these cells are occupied by several millimeters of sealant (>6 mm), making it difficult to produce small batteries with high energy density. Finally, using origami folding, Song *et al.* reported that LIBs packaged in aluminized polypropylene films and sealed by hot pressing could be transformed from planar to three-dimensional (3D) architectures.[19] However, it is difficult to generate compact 3D batteries in arbitrary motifs by folding alone.

Here, we report an integrated design and fabrication method for creating high-power aqueous Zn-ion batteries (ZIBs) in customized geometries by combining electrospinning, laser micromachining, and 3D printing techniques.[22−28] Aqueous ZIBs offer several advantages including high-rate performance

Received: April 12, 2018
Accepted: November 5, 2018
Published: November 5, 2018






DOI: 10.1021/acsnano.8b02744
ACS Nano XXXX, XXX, XXX−XXX

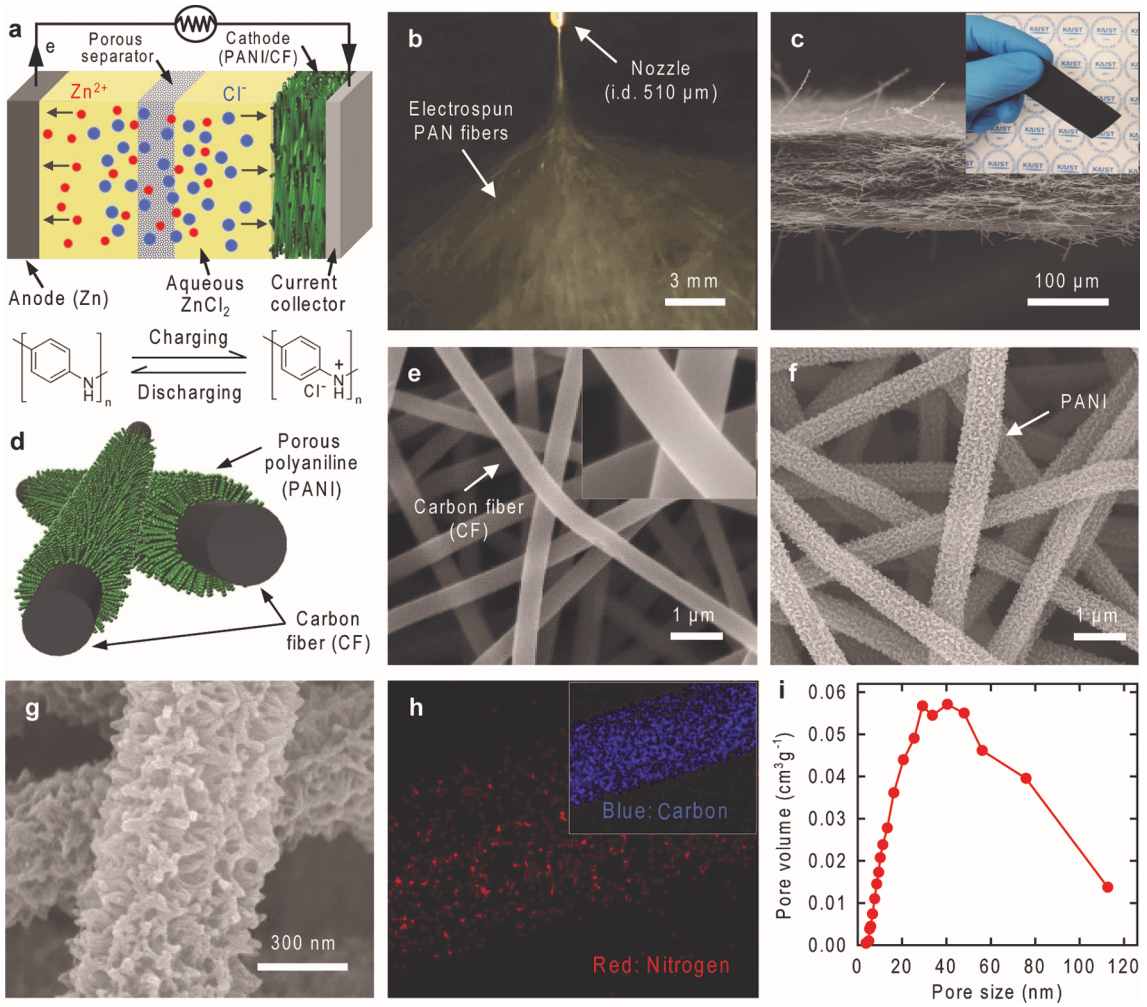


**Figure 1. ZIB and PANI/CF cathodes. (a) Schematic illustration of ZIB configuration and electrochemical reaction of PANI as cathode material. (b) Optical image captured during electrospinning of a PAN (12.5 wt %) solution at 15 kV. (c) Cross-sectional SEM image and optical image (inset) of a flexible 3D CF conductive mat produced by carbonization of the electrospun PAN fiber mat. (d) Schematic diagram illustrating the PANI/CF cathode synthesized by *in situ* polymerization in an aqueous aniline solution. (e) SEM images of the CF mat before PANI coating. The inset shows a high-magnification image. (f) Low- and (g) high-magnification SEM images of the CF mat after PANI coating. (h) Elemental maps of a representative PANI/CF cathode measured by high-angle, annular dark-field scanning TEM image (HAADF-STEM). (i) Pore size distribution of the PANI/CF cathode.**

comparable to supercapacitors, superior stability against oxygen and moisture, and glovebox-free fabrication.[27] Specifically, our aqueous ZIBs are composed of a polyaniline (PANI)-coated carbon fiber (CF) cathode, a porous separator, and a zinc (Zn) anode (Figure 1a). We utilize a stereolithography (SLA) to create custom packages, for example, simple can and lid or more complex 3D geometries, as needed. Notably, although the SLA technique has been widely used in many fields for prototyping custom-shaped complex plastic structures with ~100 $\mu$m resolution, its potential to produce customized battery packages has yet to be explored. Cathode materials with high surface area and good conductivity are essential for producing high-rate ZIBs; thus, we first synthesized a freestanding CF mat as a 3D current collector *via* electrospinning route (Figure 1b,c).[26] Next, conductive polymer, PANI, an effective cathode material for Zn-PANI batteries, was conformally coated on a CF mat to yield the desired PANI-coated CF cathode (Figure 1d).[27] We used laser micromachining to produce cell components (electrodes, separator, and terminals) in the requisite shapes for infilling the SLA-printed packages. The electrochemical performances of aqueous PANI/CF cathodes, Zn-PANI cells, and battery packs were characterized. We fabricated custom ZIBs in different form factors, including square, circular H-, and ring shapes. We then demonstrated a wearable photosensor by conformally integrating a ring-shaped battery pack with electronic components to highlight the design flexibility afforded by our method. Finally, we explored other cell chemistries, including graphene (GP) supercapacitors and Zn-$MnO_2$ batteries in both small and scalable form factors to demonstrate its broad applicability.

## RESULTS AND DISCUSSION

**Synthesis of PANI-Coated CF Cathodes.** The fabrication process used to produce the PANI/CF cathodes is highlighted in Figure S1 along with their microstructural evolution. First, we create a nonwoven mat of polyacrylonitrile (PAN) fibers (*ca.* 1 to 1.5 $\mu$m in diameter, Figure S1b) by electrospinning of a PAN solution (Figure 1b). These PAN mats are stabilized at 270 °C for 1 h in air to avoid deformation (or melting) during their subsequent carbon-


DOI: 10.1021/acsnano.8b02744
*ACS Nano* XXXX, XXX, XXX−XXX

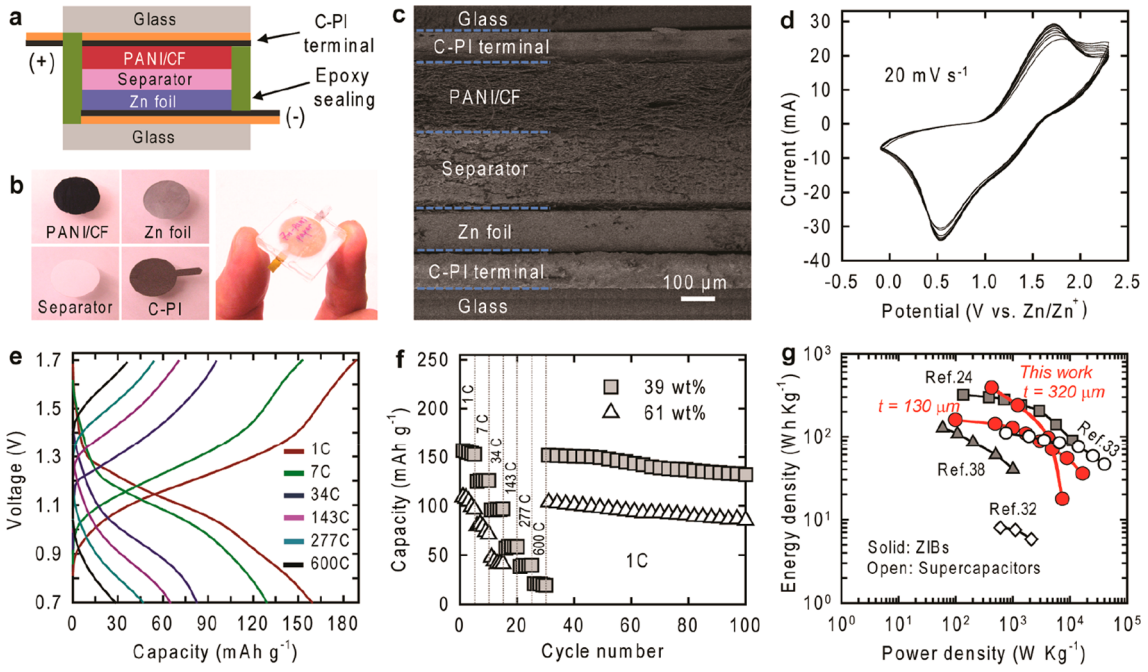


**Figure 2. Electrochemical properties of Zn-PANI cells. (a) Schematic diagram illustrating a Zn-PANI cell configuration. (b) Optical images of cell components (cathode, anode, separator, and terminal) prepared by laser micromachining and an assembled Zn-PANI cell. (c) Cross-sectional SEM image showing the individual layers within a Zn-PANI cell. (d) Cyclic voltammograms of the Zn-PANI cell measured at a scan rate of 20 mV $s^{-1}$. (e) Charge−discharge curves of the Zn-PANI cell of varying C rates. (f) Cyclability for the Zn-PANI cells with different PANI loading cycled between 0.7 and 1.7 V at various C rates. (g) Ragone plot of these Zn-PANI cells of different cathode thickness (130 and 320 $\mu$m) shown alongside other high-performance ZIBs and supercapacitors reported previously.[24,32,33,38]**

ization at 900 °C for 2 h in argon. Dehydrogenation and cyclization of PAN mats occur during the initial heating step, resulting in the stabilized PAN fibers with diameters ranging from approximately 500−800 nm (Figure S1c). Upon carbonization at 900 °C for 2 h in argon, CF mats with an average diameter of 370 nm and thickness of 130 $\mu$m are produced (Figure 1c,e). Their measured sheet resistance is approximately 20 Ω $sq^{-1}$. These CF mats serve as flexible, conductive current collectors in 3D architectures.[29]

We conformally coated these 3D CF architectures with highly porous conductive polymer (Figure 1d), PANI, which is known to be an effective cathode material for ZIBs and supercapacitors.[30−33] Before PANI coating, the surface of carbon fiber (CF) mats was activated by $HNO_3$ treatment. Previously, we have observed an increase of several functional groups such as carbonyl (C═O), ether (C−O), and carboxyl (O−C═O) groups on the surface of CF mat after $HNO_3$ treatment.[34] These functional groups facilitate subsequent *in situ* polymerization of aniline monomers by interacting with the nitrogen atoms in the −NH− group of PANI backbone through hydrogen bonds.[35,36] Specifically, a thin and highly porous PANI layer (Figure 1f,g) with a thickness of ∼150 nm is deposited onto the CFs by carrying out an *in situ* polymerization process in an aqueous aniline solution held at −20 °C in the presence of hydrochloric acid, an oxidant, ammonium persulfate, and lithium chloride as an inhibitor, which lowers the freezing point (Figure S2). By optimizing the reaction time and number of coated layers (Figures S3 and S4), we produced PANI/CF cathodes that contained a PANI loading of 30−80 wt %, whose sheet resistance is roughly 400 Ω $sq^{-1}$. The TEM image (Figure S1g) and corresponding elemental maps (Figure 1h) reveal that the nitrogen atoms are uniformly distributed, suggesting that a homogeneous PANI overlayer is formed on the entire surface of the flexible CF mat. The X-ray diffraction (XRD) and Fourier-transform infrared spectroscopy (FTIR) analyses confirmed the crystalline nature and composition of our PANI/CF cathodes (Figure S5). The average pore size in the PAN/CF cathode is 40 nm (Figure 1i).

**Electrochemical Performance of PANI/CF Cathodes.** To investigate electrochemical performance of the PANI/CF cathodes, we created a simple aqueous Zn-PANI cell stacked and packaged between two glass substrates sealed with epoxy (Figure 2a,b). The cell consists of a PANI/CF cathode (∼320 $\mu$m thick), Zn foil anode (125 $\mu$m thick), glass fiber separator (250 $\mu$m thick), and carbon (17 $\mu$m thick)-laminated polyimide (PI, 60 $\mu$m thick) terminals as current collectors (Figure 2c). Note, we cannot use coin cell (stainless steel) packaging for this ZIB cell, because $Cl^-$ present in the aqueous electrolyte (1 M $ZnCl_2$) accelerates their anodic dissolution. By contrast, carbon-laminated PI (hereafter, C-PI) terminals are stable with respect to both the cathode and anode materials in these cells. Cyclic voltammetry (CV) of this Zn-PANI cell is measured in an aqueous $ZnCl_2$ (1 M) solution at a scan rate of 20 mV $s^{-1}$ (Figure 2d). The cathodic and anodic peaks near 0.5 and 1.6 V (*vs* $Zn/Zn^{2+}$) are associated with the deposition and dissolution of $Zn^{2+}$ ions onto and from the Zn anode. The CV curves exhibit no significant changes after 10 cycles, indicating the reversible redox behavior of the PANI. $Zn^{2+}$ ions are deposited onto the metallic Zn anode from the electrolyte solution, and simultaneously, the surface of PANI is oxidized by doping of $Cl^-$ ions during charge (Figure 1a). The opposite reaction occurs during discharge.[37]

We measured the charge/discharge curves of the aqueous Zn-PANI cell between 0.7 and 1.7 V at different C rates (Figure 2e). The battery exhibits a discharge capacity of 165 mAh $g^{-1}$ at 1 C and is even capable of operating at 600 C.



DOI: 10.1021/acsnano.8b02744
ACS Nano XXXX, XXX, XXX−XXX

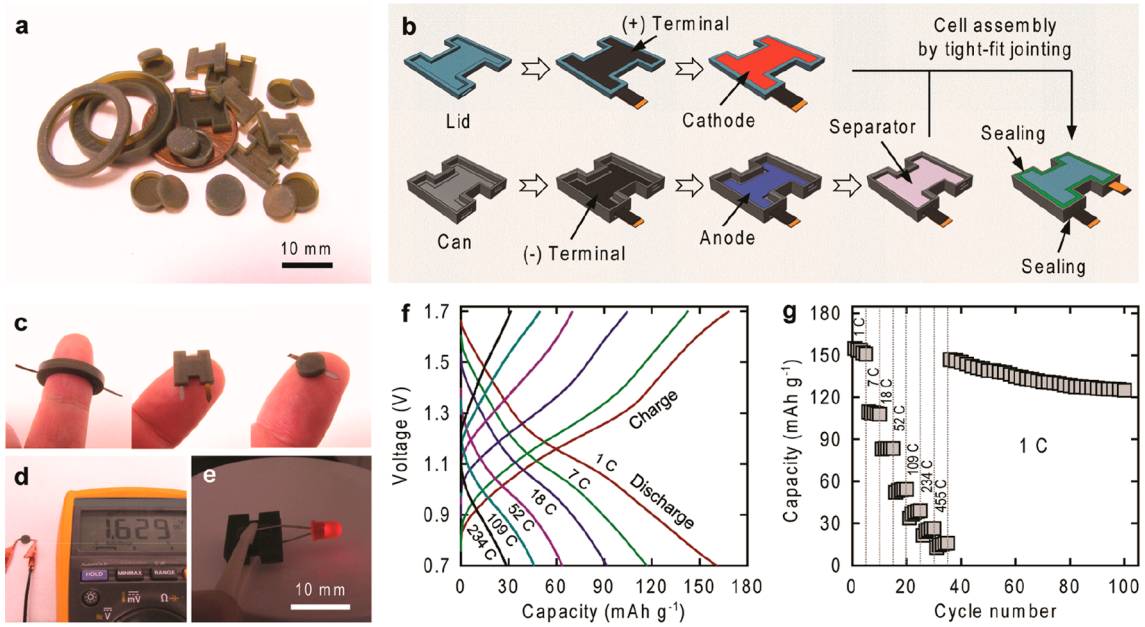


**Figure 3. Fabrication of Zn-PANI cell in arbitrary geometries. (a) Optical image of printed can and lid structures in different packaging shapes and sizes. (b) Schematic diagrams illustrating the integrated assembly process for a representative H-shaped Zn-PANI battery. (c) Optical images of assembled Zn-PANI batteries in ring-, H-, and cylindrical shapes. (d) Optical image of the spherical Zn-PANI battery showing the cell voltage. (e) Optical image of a LED operated by two H-shaped Zn-PANI batteries connected in serial. (f) Rate capability and (g) cycling performance of a cylindrical Zn-PANI battery measured within a voltage window of 0.7−1.7 V at different C rates.**

Capacity retention characteristics of more than 50% at 34 C and 19% at 600 C are observed, corresponding to charge and discharge times of 106 and 6 s, respectively. This ultrafast rate capability stems from the rational design of the PANI/CF cathode, that is, the highly conductive and 3D structured CF mat facilitates fast electron transfer even for relatively thick PANI-CF mats (~320 um). Furthermore, the porous PANI/CF architecture enables fast ion diffusion within cathode layers. We also measured the cyclic stability of the Zn-PANI cells with PANI loadings of 39 and 61 wt % at different C rates (Figure 2f). Both cells regained nearly their initial capacities at 1 C after cycling ~100 times with only a modest capacity fade (~20%). Notably, the ZIB cell with thicker PANI/CF cathodes (61 wt % PANI, 320 $\mu$m thick) exhibited a lower capacity (120 mAh $g^{-1}$) at 1 C and a higher capacity fade at higher C rates (Figure 2f). The accompanying Ragone plot reveals that the Zn-PANI batteries possess comparable energy and power densities to other high-performance ZIBs and supercapacitors reported in the literature (Figure 2g).[24,32,33,38] A cell with a 130 $\mu$m-thick PANI/CF cathode delivered a maximum energy density and power density of 159 Wh $kg^{-1}$ and 16.7 kW $kg^{-1}$, respectively. Although higher energy density of 389 Wh $kg^{-1}$ is observed for cells with a thicker (320 $\mu$m) PANI/CF cathode, this value decreases sharply with increasing power density. We also compared our Zn-PANI cells with other cell chemistries, including supercapacitor, alkaline, lead acid, nickel zinc (NiZn), silver zinc (AgZn), and LIBs in Figure S6, which further highlights superior electrochemical performance of our Zn-PANI cells at high C rates.

**Fabrication of Aqueous Zn-PANI Cells in Arbitrary Form Factors.** To demonstrate facile assembly of aqueous Zn-PANI cells in arbitrary geometries, we created polymer packaging structures (can and lid) by SLA (Figure 3a), including those in ring (i.d. 14 mm, o.d. 21 mm, 1.7 mm thick), H- (10 × 10 × 1.7 $mm^3$), and cylindrical (7 mm diameter, 1.7 mm thick) shapes. Note, these cell thicknesses correspond to fully packaged ZIBs. While a minimum wall thickness of ~100 $\mu$m can be produced, we created slightly thicker structures (>300 $\mu$m) to provide sufficient mechanical strength. Other cell components, including the PANI/CF cathode, Zn foil anode, paper separator (100 $\mu$m thick), and C-PI terminals are laser micromachined into the desired forms with a resolution of ~20 $\mu$m (Figure S7). Figure 3b shows schematic illustrations of the assembly process for a representative H-shaped cell. First, a C-PI terminal and PANI/CF cathode are inserted into the printed lid structure, while the laser-cut C-PI terminal, Zn foil anode, and paper separator are separately inserted into the can structure. The H-shaped cell is produced by combining the lid and can structures, followed by electrolyte filling by applying vacuum in $ZnCl_2$ (1 M) solution. The vacuum process is required in electrolyte filling to remove bubbles in the cell. The final assembled H-shaped cell is then sealed with an epoxy resin, which fills the groove and wells formed at the interface between the can and lid structures (Figure S8).

Figure 3c shows optical images of the aqueous Zn-PANI cells in ring, H, and cylindrical shapes. The cylindrical cell has a potential of 1.69 V after charging (Figure 3d). Two H-shaped cells connected in series can turn on a red LED (Figure 3e). The rate performance and cyclic behavior of a fully assembled cylindrical cell are measured in a voltage window of 0.7−1.7 V at different C rates. The cell exhibits a discharge capacity of 162 mAh $g^{-1}$ at 1 C, while maintaining a capacity retention of 56% at 18 C and 18% at 234 C, respectively (Figure 3f). The cell capacity decreases with increasing discharge rate, but recovers nearly its initial capacity when cycled at 1 C (Figure 3g), that is, only ~15% capacity fade is observed after 100 cycles. While it is difficult to package LIBs in plastics with organic electrolytes due to oxygen and moisture permeation, this method is suitable for aqueous-based ZIBs.



DOI: 10.1021/acsnano.8b02744
ACS Nano XXXX, XXX, XXX−XXX

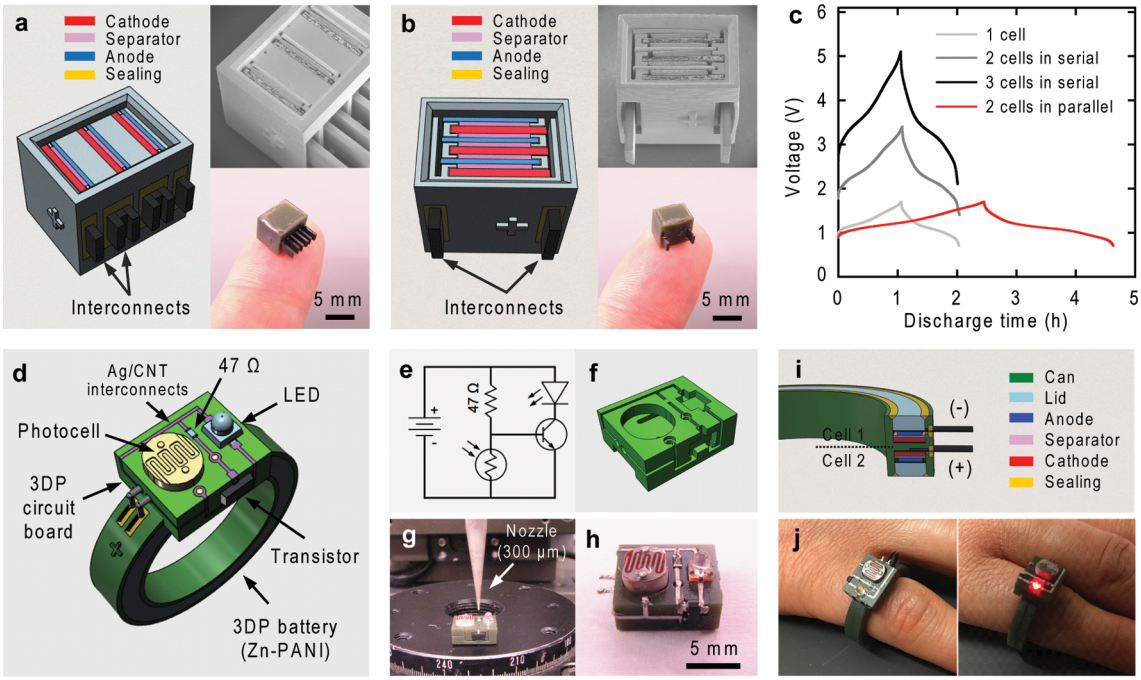


**Figure 4. Fabrication of Zn-PANI battery packs for shape conformable integration. Schematic diagrams and corresponding images of Zn-PANI battery packs with stacked electrodes housed within 3D printed packages that are connected in (a) serial and (b) parallel. (c) Charge–discharge curves of the Zn-PANI battery packs measured as a function of discharge time. (d) Schematic and (e) circuit diagrams of a wearable photosensor with a ring-shape Zn-PANI battery and a 3D printed circuit board. (f) Schematic diagram of the 3D printed circuit board before placing electronic components. (g) Optical image taken during direct writing of a conductive Ag/CNT ink within the interconnect trenches on the 3D printed circuit board. (h) Optical image of the 3D printed circuit board after electrical interconnection. (i) Schematic diagram illustrating a ring-shape Zn-PANI battery configuration that is shape conformably wearable on a pinky finger. (j) Optical images of the wearable photosensor on a pinky finger in bright (left) and dark (right) conditions.**

**Aqueous Zn-PANI Battery Packs for Integration with Wearable Electronics.** The ability to create customized battery packs with specified voltage and capacity is crucial for numerous applications. We assembled an aqueous Zn-PANI battery pack (~0.3 $cm^3$) with vertically stacked electrodes that can be interconnected, as needed (Figure 4a–c). As an exemplar, we printed packaging structures in rectangular shapes (7.7 mm wide, 6.6 mm long, and ~6.4 mm thick) with partitioned slots, in which we inserted laser-cut PANI/CF cathodes (400 $\mu$m thick), paper separators (200 $\mu$m thick), Zn foil anodes (250 $\mu$m thick), and graphite terminals (500 $\mu$m thick). Next, we filled the assembled battery pack with an aqueous electrolyte (1 M $ZnCl_2$), attached the printed lid, sealed it with epoxy, and connected it in series (Figure 4a) or parallel (Figure 4b). When three cells are interconnected in series, their voltage is enhanced by a factor of 3 over the individual cell voltage, yet they possess a similar discharge time at a given current (Figure 4c). When two battery packs are interconnected in parallel, their cell capacity and discharge time are doubled for a given current (Figure 4c). We investigated the rate performance, cyclability, and Coulombic efficiency of these interconnected cells in parallel and serial. Similar to performance of single cell Zn-PANI batteries, the interconnected battery packs exhibit high rate performance and cyclability (Figure S9). Columbic efficiencies of the battery packs with parallel and serial interconnection were measured as high as 98% and only decrease to ~92% after cycling 50 times with different C rates (Figure S9).

As a final demonstration, we created an integrated wearable photosensor that consists of electronic components, including a ring-shaped battery, a photocell, a resistor (47 Ω), a transistor (MMBT3904L), and a red LED (Figure 4d). The circuit diagram of the sensor device is shown in Figure 4e. First, we printed a circuit board (8.2 × 9.8 × 3.7 $mm^3$) with cavities and trenches (0.3 mm wide and deep) to house the surface-mount electronic components and conductive interconnects, respectively (Figure 4f). The components were manually inserted into the cavities, and then conductive interconnects were printed by direct writing of a Ag/CNT ink into the trenches using a 300 $\mu$m nozzle (Figure 4g,h).[39,40] The printed Ag/CNT interconnects exhibit an electrical conductivity of ~2 × $10^4$ S $cm^{-1}$ after annealing at 80 °C for 1 h. Next, we created a shape conformable and wearable aqueous Zn-PANI battery pack in the form of a ring-shaped (i.d. 16 mm, o.d. 22 mm, 4.1 mm thick) (Figure 4i), which consists of two Zn-PANI cells that are interconnected in serial to operate the circuit at 3 V. This wearable device turns on the red LED when the photocell detects a certain level of darkness (Figure 4j).

Our integrated design and fabrication strategy can be readily extended to other cell chemistries (Figure 5). We fabricated a thin square-shaped (10 × 10 × 2 $mm^3$) GP-based supercapacitor using electrodes synthesized by GP ink coating on PI substrate, followed by xenon flash lamp-assisted optical sintering (Figure 5a,b).[41] The cell fabrication process is illustrated in Figure S10. The galvanostatic charge and discharge curves confirmed the capacitive behavior of GP-based supercapacitor (Figure 5c). Notably, the device performance can be further improved by optimizing electrode thickness, surface area, and conductivity. To demonstrate other ZIB chemistries, we synthesized $MnO_2$-coated CF cathodes by co-precipitation of manganese acetate and potassium perman-


DOI: 10.1021/acsnano.8b02744
ACS Nano XXXX, XXX, XXX–XXX

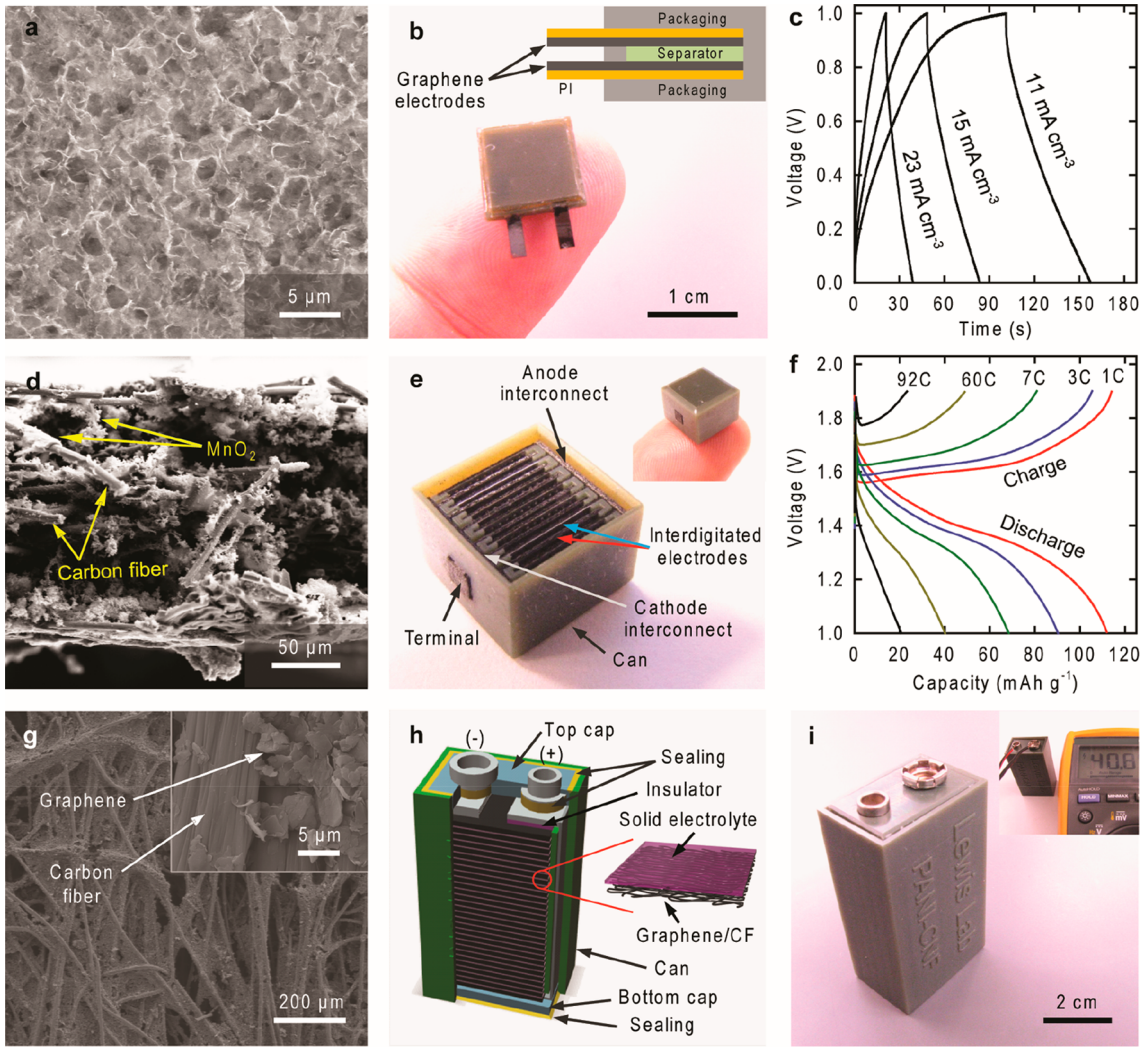


**Figure 5. Extension of our approach to other electrochemical cells. (a) SEM image of a GP electrode created by GP ink coating on a PI substrate, followed by photonic annealing. (b) Optical image and schematic diagram (inset) of a GP supercapacitor (10 × 10 × 2 $mm^3$) composed of SLA-printed packaging, GP electrodes, a paper separator, and an aqueous $H_3PO_4$ (1 M) electrolyte. (c) Galvanostatic charge−discharge curves of the GP supercapacitor at different current densities. (d) SEM image of a $MnO_2$-coated CF cathode synthesized by coprecipitation of manganese acetate and potassium permanganate solutions. (e) Optical images of a Zn-$MnO_2$ battery (9 × 9 × 6.3 $mm^3$) composed of SLA-printed packaging, interdigitated electrodes ($MnO_2$/CF cathode, Zn foil anode), and an aqueous $ZnSO_4$ (1 M) electrolyte. The inset shows the Zn-$MnO_2$ battery after sealing. (f) Rate performance of the Zn-$MnO_2$ battery at different C rates. (g) SEM images of a GP/CF electrode synthesized by GP ink coating on CF sheet, followed by annealing at 100 °C. (h) Schematic diagram illustrating an E-size (17.5 × 26.5 × 48.5 $mm^3$) prismatic supercapacitor composed of SLA-printed packaging, 54 GP/CF electrodes coated with solid electrolyte ($H_3PO_4$/PVA) on one side, and stainless steel terminals. (i) Optical images of the prismatic supercapacitor after assembly. The inset shows cell voltage (40 V).**

ganate solutions (Figure 5d). A high-rate performance square-shaped (9 × 9 × 6.3 $mm^3$) Zn-$MnO_2$ battery was successfully produced by stacking interdigitated electrodes using Zn foil anodes, $MnO_2$/CF cathodes, and an aqueous Zn $SO_4$ (1 M) electrolyte (Figure 5e,f and Figure S11). The cycling performance of this battery at different C rates is reported in Figure S12. To demonstrate scalability, we created an E-size (17.5 × 26.5 × 48.5 $mm^3$) prismatic supercapacitor composed of SLA-printed packaging, 54 GP/CF electrodes coated with solid electrolyte ($H_3PO_4$/PVA) on one side, and stainless steel terminals (Figure 5g,h). A stable operation of high voltage (40 V) prismatic cell was observed (Figure 5i).

## CONCLUSIONS

We developed high-power and shape conformal aqueous ZIB packs by exploiting an integrated design and fabrication method. Specifically, we have successfully demonstrated high-rate aqueous ZIBs in various form factors, including ring, H-, cylindrical, and other polygonal geometries. As further exemplars, we produced small (~8 mm) ZIB packs with adjustable voltage and capacity in customized geometries that could be connected in series or parallel as well as wearable devices, in which customized ZIBs are readily integrated along with surface mount electronic components and printed conductive interconnects. We have focused on ZIBs and supercapacitors with aqueous electrolytes due to their outstanding electrochemical stability against oxygen and moisture. Further advances are needed to enable high-


DOI: 10.1021/acsnano.8b02744
ACS Nano XXXX, XXX, XXX−XXX

throughput production of customized ZIBs, which we envision being made in digital microfactories equipped with additive and subtractive patterning tools along with automated pick-and-place capabilities.

## EXPERIMENTAL SECTION

**Synthesis of PANI/CF Cathodes.** The cathodes are prepared by electrospinning, followed by stabilization, carbonization, and subsequent polyaniline (PANI) coating. First, an electrospinning solution composed of polyacrylonitrile (PAN, 12.5 wt %, $M_w$ = 150,000 g $mol^{-1}$, Aldrich) in *N*,*N*-dimethylformamide (DMF, Aldrich) is prepared by stirring on a hot plate at 60 °C for 12 h. This solution is then loaded into a plastic syringe, placed at a distance of 20 cm from a stainless foil collector wrapped on a cylinder of 8 cm in diameter. During electrospinning, a voltage of 15.5 kV is applied using a high-voltage DC power supply through the tip of a stainless steel needle (21 gauge) connected to the syringe. The flow rate is adjusted to 1.2 mL $h^{-1}$, and the rotating speed of the cylindrical collector is 100 rpm. Electrospinning is carried out at room temperature at 30% RH. The as-spun fiber mat (~320 $\mu$m thick) is detached from the collector, heated to 270 °C at a ramp of 5 °C $min^{-1}$ in air and held for 1 h, and then heated at 900 °C at a ramping rate of 3 °C $min^{-1}$ in argon and held for 2 h. The resulting carbon fiber (CF) mat is hydrophobic. To increase its wettability to water, the CF mat is immersed in a nitric acid solution (70 wt % $HNO_3$, Kanto Chem.) for 30 min at 50 °C. Finally, a PANI coating layer is deposited onto the activated CF mat by an *in situ* chemical polymerization process. Specifically, two solutions are used for this process. First, an aqueous aniline solution is prepared by mixing 0.19 g aniline monomer, 5 g hydrochloric acid (HCl, 35% in water), and 8 g lithium chloride in 50 mL water. Separately, an oxidant solution is prepared by mixing 0.02 g ammonium persulfate ($(NH_4)_2S_2O_8$, Kanto Chem.) and 1.6 g lithium chloride in 10 mL water. Those two solutions are cooled to −20 °C. The PANI coating is carried out by immersing the CF mats within the mixed solutions and holding it for ~48 h at −20 °C. PANI-coated CF (PANI/CF) cathodes with 29−80 wt % PANI content are produced by repeating the coating process, as needed.

**Fabrication of Zn-PANI Batteries.** ZIB batteries are produced in simple and customized geometries. The cathodes (PANI/CF mats ~320 $\mu$m thick), separators (glass fiber in 250 $\mu$m or paper in 100−250 $\mu$m thick), anodes (Zn foil, 125−250 $\mu$m thick), and carbon (17 $\mu$m)-laminated polyimide (PI, 60 $\mu$m thick) terminals are prepared in desired shapes and sizes by laser micromachining (HurryScan, 355 nm, spot size 10−26 $\mu$m). Simple ZIBs are made by sandwiching the cell components in two glass substrates, followed by epoxy sealing. The customized ZIBs are assembled within 3D printed polymer cans, and lids fabricated by stereolithography (SLA) (EnvisionTech, Aureus). Specifically, a C-PI terminal and PANI/CF cathode are inserted in the lid structure, while a C-PI terminal, Zn foil anode, and paper separator are inserted in the can structure. Next, the cell is then assembled by jointing the can and lid structures together, followed by electrolyte filling by applying vacuum in an aqueous $ZnCl_2$ (1 M) solution, and then sealing with an epoxy resin, which cures in 30 min at room temperature.

**Physical, Chemical, and Electrical Characterization.** The sheet resistance of the PANI/CF cathodes is measured using a four-point probe apparatus (MS-Tech8000). The microstructure and morphology of PAN, CF, and PANI/CF fibers are characterized using field emission SEM (Nova 230, FEI) operating at 10 kV. The crystalline structures of CF and PANI/CF are analyzed using an X-ray powder diffractometer (XRD, D/MAX-2500, Rigaku) with Cu K$\alpha$ radiation ($\lambda$= 1.54056 Å) between 10° and 90° at a scan rate of 3° $min^{-1}$. FTIR spectra of CF and PANI/CF are obtained using a FT-IR spectrometer (Nicolet iS50, Thermo Fisher Scientific Instrument). Finally, the morphology of PANI/CF fibers are observed using a Cs-corrected scanning TEM (JEM-ARM200F, JEOL) at an accelerating voltage of 300 kV.

**Electrochemical Measurements.** A multimeter (Fluke 179) is used to measure cell voltage. All electrochemical measurements are carried out for the fully assembled batteries and battery packs in ambient air using the potentiostat (VMP-3, Biologic Co.). Cyclic voltammetry (CV) is measured in an aqueous $ZnCl_2$ (1 M) solution at a scan rate of 20 mV $s^{-1}$. To investigate rate capability and cyclability, charge/discharge tests are performed at a voltage window of 0.7−1.7 V of varying C rates using the aqueous $ZnCl_2$ (1 M) solution. The electrochemical impedance spectroscopy (ZIVE SPI, WonATech) are measured in a frequency ranging from 1 to 10 MHz with AC voltage amplitude of 5 mV.

## ASSOCIATED CONTENT

### Supporting Information

The Supporting Information is available free of charge on the ACS Publications website at DOI: 10.1021/acsnano.8b02744.

Experimental details of PANI coating, characterizations (SEM, TEM, XRD, FTIR) of PANI-coated CFs, Ragone plot of Zn-PANI cells, optical images of the 3D printed cell components, and schematic illustrations of an H-shaped Zn-PANI battery and the fabrication process for a Zn-$MnO_2$ battery (PDF)

## AUTHOR INFORMATION


### Corresponding Authors

*E-mail: idkim@kaist.ac.kr.

*E-mail: jalewis@seas.harvard.edu.

### ORCID

Sunho Jeong: 0000-0002-5969-1614

Il-Doo Kim: 0000-0002-9970-2218

Jennifer A. Lewis: 0000-0002-0280-2774

### Author Contributions

#These authors contributed equally to this work.


### Notes

The authors declare no competing financial interest.

## ACKNOWLEDGMENTS

This work was supported by the Global Research Laboratory Program of the National Research Foundation (NRF) funded by Ministry of Science, Information and Communication Technologies and Future Planning (NRF-2015K1A1A2029679), and by the Soft Robotics Platform in the Wyss Institute for Biologically Inspired Engineering. We gratefully acknowledge the use of facilities at the Center for Nanoscale Systems (CNS) at Harvard University. We also gratefully acknowledge Professor Robert Wood for use of his laser micromachining equipment at Harvard University. I.-D.K. thanks the National Research Foundation of Korea (NRF), grant no. 2014R1A4A1003712 (BRL Program) and Wearable Platform Materials Technology Center (WMC) funded by the National Research Foundation of Korea (NRF) Grant of the Korean Government (MSIP) (no. 2016R1A5A1009926). Finally, J.A.L. thanks the GETTYLAB for their generous support of our work.

## REFERENCES

(1) Ha, M.; Lim, S.; Ko, H. Wearable and Flexible Sensors for User-Interactive Health-Monitoring Devices. *J. Mater. Chem. B* **2018**, *6*, 4043−4064.

(2) Sun, K.; Wei, T.-S.; Ahn, B. Y.; Seo, J. Y.; Dillon, S. J.; Lewis, J. A. 3D Printing of Interdigitated Li-Ion Microbattery Architectures. *Adv. Mater.* **2013**, *25*, 4539−4543.

(3) Long, J. W.; Dunn, B.; Rolison, D. R.; White, H. S. Three-Dimensional Battery Architectures. *Chem. Rev.* **2004**, *104*, 4463−4492.



DOI: 10.1021/acsnano.8b02744
*ACS Nano* XXXX, XXX, XXX−XXX

(4) Zamarayeva, A. M.; Ostfeld, A. E.; Wang, M.; Duey, J. K.; Deckman, I.; Lechene, B. P.; Davies, G.; Steingart, D. A.; Arias, A. C. Flexible and Stretchable Power Sources for Wearable Electronics. *Sci. Adv.* **2017**, *3*, e1602051.
(5) Ma, K. Y.; Chirarattananon, P.; Fuller, S. B.; Wood, R. J. Controlled Flight of a Biologically Inspired, Insect-Scale Robot. *Science* **2013**, *340*, 603−607.
(6) Wehner, M.; Truby, R. L.; Fitzgerald, D. J.; Mosadegh, B.; Whitesides, G. M.; Lewis, J. A.; Wood, R. J. An Integrated Design and Fabrication Strategy for Entirely Soft, Autonomous Robots. *Nature* **2016**, *536*, 451−455.
(7) Laschi, C.; Mazzolai, B.; Cianchetti, M. Soft robotics: Technologies and Systems Pushing the Boundaries of Robot Abilities. *Sci. Robot.* **2016**, *1*, eaah3690.
(8) Wang, Z. L.; Chen, J.; Lin, L. Progress in Triboelectric Nanogenerators as a New Energy Technology and Self-Powered Sensors. *Energy Environ. Sci.* **2015**, *8*, 2250−2282.
(9) Dagdeviren, C.; Su, Y.; Joe, P.; Yona, R.; Liu, Y.; Kim, Y. S.; Huang, Y.; Damadoran, A. R.; Xia, J.; Martin, L. W.; Huang, Y.; Rogers, J. A. Conformable Amplified Lead Zirconate Titanate Sensors with Enhanced Piezoelectric Response for Cutaneous Pressure Monitoring. *Nat. Commun.* **2014**, *5*, 4496.
(10) Albano, F.; Chung, M. D.; Blaauw, D.; Sylvester, D. M.; Wise, K. D.; Sastry, A. M. Design of an Implantable Power Supply for an Intraocular Sensor, Using POWER (Power Optimization for Wireless Energy Requirements). *J. Power Sources* **2007**, *170*, 216−224.
(11) Lee, Y. H.; Kim, J. S.; Noh, J.; Lee, I.; Kim, H. J.; Choi, S.; Seo, J.; Jeon, S.; Kim, T. S.; Lee, J. Y.; Choi, J. W. Wearable Textile Battery Rechargeable by Solar Energy. *Nano Lett.* **2013**, *13*, 5753−5761.
(12) Pu, X.; Li, L.; Song, H.; Du, C.; Zhao, Z.; Jiang, C.; Cao, G.; Hu, W.; Wang, Z. L. A Self-Charging Power Unit by Integration of a Textile Triboelectric Nanogenerator and a Flexible Lithium-Ion Battery for Wearable Electronics. *Adv. Mater.* **2015**, *27*, 2472−2478.
(13) Guo, H.; Yeh, M. H.; Lai, Y. C.; Zi, Y.; Wu, C.; Wen, Z.; Hu, C.; Wang, Z. L. All-in-One Shape-Adaptive Self-Charging Power Package for Wearable Electronics. *ACS Nano* **2016**, *10*, 10580−10588.
(14) Sun, H.; Zhang, Y.; Zhang, J.; Sun, X.; Peng, H. Energy Harvesting and Storage in 1D Devices. *Nat. Rev. Mater.* **2017**, *2*, 17023.
(15) Wang, X. F.; Lu, X. H.; Liu, B.; Chen, D.; Tong, Y. X.; Shen, G. Z. Flexible Energy-Storage Devices: Design Consideration and Recent Progress. *Adv. Mater.* **2014**, *26*, 4763−4782.
(16) Kwon, Y. H.; Woo, S. W.; Jung, H. R.; Yu, H. K.; Kim, K.; Oh, B. H.; Ahn, S.; Lee, S. Y.; Song, S. W.; Cho, J.; Shin, H. C.; Kim, J. Y. Cable-Type Flexible Lithium Ion Battery Based on Hollow Multi-Helix Electrodes. *Adv. Mater.* **2012**, *24*, 5192−5197.
(17) Xu, S.; Zhang, Y. H.; Cho, J.; Lee, J.; Huang, X.; Jia, L.; Fan, J. A.; Su, Y. W.; Su, J.; Zhang, H. G.; Cheng, H. Y.; Lu, B. W.; Yu, C. J.; Chuang, C.; Kim, T. I.; Song, T.; Shigeta, K.; Kang, S.; Dagdeviren, C.; Petrov, I.; Braun, P. V.; Huang, Y. G.; Paik, U.; Rogers, J. A. Stretchable Batteries with Self-Similar Serpentine Interconnects and Integrated Wireless Recharging Systems. *Nat. Commun.* **2013**, *4*, 1543.
(18) Gaikwad, A. M.; Zamarayeva, A. M.; Rousseau, J.; Chu, H. W.; Derin, I.; Steingart, D. A. Highly Stretchable Alkaline Batteries Based on an Embedded Conductive Fabric. *Adv. Mater.* **2012**, *24*, 5071−5076.
(19) Song, Z. M.; Ma, T.; Tang, R.; Cheng, Q.; Wang, X.; Krishnaraju, D.; Panat, R.; Chan, C. K.; Yu, H. Y.; Jiang, H. Q. Origami Lithium-Ion Batteries. *Nat. Commun.* **2014**, *5*, 3140.
(20) Kim, S. H.; Choi, K. H.; Cho, S. J.; Choi, S.; Park, S.; Lee, S. Y. Printable Solid-State Lithium-Ion Batteries: A New Route toward Shape-Conformable Power Sources with Aesthetic Versatility for Flexible Electronics. *Nano Lett.* **2015**, *15*, 5168−5177.
(21) Lee, Y. H.; Kim, J. S.; Noh, J.; Lee, I.; Kim, H. J.; Choi, S.; Seo, J.; Jeon, S.; Kim, T. S.; Lee, J. Y.; Choi, J. W. Wearable Textile Battery Rechargeable by Solar Energy. *Nano Lett.* **2013**, *13*, 5753−5761.
(22) Cai, Z. J.; Guo, J.; Yang, H. Z.; Xu, Y. Electrochemical Properties of Electrospun Poly(5-Cyanoindole) Submicron-Fibrous Electrode for Zinc/Polymer Secondary Battery. *J. Power Sources* **2015**, *279*, 114−122.
(23) Zhijiang, C.; Chengwei, H. Study on the Electrochemical Properties of Zinc/Polyindole Secondary Battery. *J. Power Sources* **2011**, *196*, 10731−10736.
(24) Xu, C.; Chen, Y.; Shi, S.; Li, J.; Kang, F.; Su, D. Secondary Batteries with Multivalent Ions for Energy Storage. *Sci. Rep.* **2015**, *5*, 14120.
(25) Pan, H. L.; Shao, Y. Y.; Yan, P. F.; Cheng, Y. W.; Han, K. S.; Nie, Z. M.; Wang, C. M.; Yang, J. H.; Li, X. L.; Bhattacharya, P.; Mueller, K. T.; Liu, J. Reversible Aqueous Zinc/Manganese Oxide Energy Storage from Conversion Reactions. *Nat. Energy* **2016**, *1*, 16039.
(26) Alfaruqi, M. H.; Gim, J.; Kim, S.; Song, J.; Jo, J.; Kim, S.; Mathew, V.; Kim, J. Enhanced Reversible Divalent Zinc Storage in a Structurally Stable Alpha-$MnO_2$ Nanorod Electrode. *J. Power Sources* **2015**, *288*, 320−327.
(27) Xu, C.; Li, B.; Du, H.; Kang, F. Energetic Zinc Ion Chemistry: The Rechargeable Zinc Ion Battery. *Angew. Chem., Int. Ed.* **2012**, *51*, 933−935.
(28) Alfaruqi, M. H.; Islam, S.; Gim, J.; Song, J.; Kim, S.; Pham, D. T.; Jo, J.; Xiu, Z.; Mathew, V.; Kim, J. A High Surface Area Tunnel-Type Alpha-$Mno_2$ Nanorod Cathode by a Simple Solvent-Free Synthesis for Rechargeable Aqueous Zinc-Ion Batteries. *Chem. Phys. Lett.* **2016**, *650*, 64−68.
(29) Jung, J. W.; Lee, C. L.; Yu, S.; Kim, I. D. Electrospun Nanofibers as a Platform for Advanced Secondary Batteries: A Comprehensive Review. *J. Mater. Chem. A* **2016**, *4*, 703−750.
(30) Ghanbari, K.; Mousavi, M. F.; Shamsipur, M. Preparation of Polyaniline Nanofibers and Their Use as a Cathode of Aqueous Rechargeable Batteries. *Electrochim. Acta* **2006**, *52*, 1514−1522.
(31) Xu, G.; Xu, D.; Zhang, J.; Wang, K.; Chen, Z.; Chen, J.; Xu, Q. Controlled Fabrication of PANI/CNF Hybrid Films: Molecular Interaction Induced Various Micromorphologies and Electrochemical Properties. *J. Colloid Interface Sci.* **2013**, *411*, 204−212.
(32) Meng, C. Z.; Liu, C. H.; Chen, L. Z.; Hu, C. H.; Fan, S. S. Highly Flexible and All-Solid-State Paper Like Polymer Supercapacitors. *Nano Lett.* **2010**, *10*, 4025−4031.
(33) Zhi, M. J.; Manivannan, A.; Meng, F. K.; Wu, N. Q. Highly Conductive Electrospun Carbon Nanofiber/$Mno_2$ Coaxial Nano-Cables for High Energy and Power Density Supercapacitors. *J. Power Sources* **2012**, *208*, 345−353.
(34) Yoon, K. R.; Shin, K.; Park, J.; Cho, S. H.; Kim, C.; Jung, J. W.; Cheong, J. Y.; Byon, H. R.; Lee, H. M.; Kim, I. D. Brush-Like Cobalt Nitride Anchored Carbon Nanofiber Membrane: Current Collector Catalyst Integrated Cathode for Long Cycle $LiO_2$ Batteries. *ACS Nano* **2018**, *12*, 128−139.
(35) Hao, Q. L.; Xia, X. F.; Lei, W.; Wang, W. J.; Qiu, J. S. Facile Synthesis of Sandwich-like Polyaniline/Boron-doped Graphene Nano Hybrid for Supercapacitors. *Carbon* **2015**, *81*, 552−563.
(36) Wang, H. L.; Hao, Q. L.; Yang, X. J.; Lu, L. D.; Wang, X. Graphene Oxide Doped Polyaniline for Supercapacitors. *Electrochem. Commun.* **2009**, *11*, 1158−1161.
(37) Zhao, Y. F.; Si, S. H.; Liao, C. A Single Flow Zinc//Polyaniline Suspension Rechargeable Battery. *J. Power Sources* **2013**, *241*, 449−453.
(38) Guerfi, A.; Trottier, J.; Boyano, I.; De Meatza, I.; Blazquez, J. A.; Brewer, S.; Ryder, K. S.; Vijh, A.; Zaghib, K. High Cycling Stability of Zinc-Anode/Conducting Polymer Rechargeable Battery with Non-Aqueous Electrolyte. *J. Power Sources* **2014**, *248*, 1099−1104.
(39) Jo, Y.; Kim, J. Y.; Kim, S. Y.; Seo, Y. H.; Jang, K. S.; Lee, S. Y.; Jung, S.; Ryu, B. H.; Kim, H. S.; Park, J. U.; Choi, Y.; Jeong, S. 3D-Printable, Highly Conductive Hybrid Composites Employing Chemically-Reinforced, Complex Dimensional Fillers and Thermoplastic Triblock Copolymers. *Nanoscale* **2017**, *9*, 5072−5084.
(40) Jo, Y.; Kim, J. Y.; Jung, S.; Ahn, B. Y.; Lewis, J. A.; Choi, Y.; Jeong, S. 3D Polymer Objects with Electronic Components


DOI: 10.1021/acsnano.8b02744
*ACS Nano* XXXX, XXX, XXX−XXX

Interconnected *via* Conformally Printed Electrodes. *Nanoscale* **2017**, *9*, 14798−14803.
(41) Li, L.; Secor, E. B.; Chen, K. S.; Zhu, J.; Liu, X. L.; Gao, T. Z.; Seo, J. W. T.; Zhao, Y. C.; Hersam, M. C. High-Performance Solid-State Supercapacitors and Microsupercapacitors Derived from Printable Graphene Inks. *Adv. Energy Mater.* **2016**, *6*, 1600909.



DOI: 10.1021/acsnano.8b02744
*ACS Nano* XXXX, XXX, XXX−XXX